Analysis of the gait generation principle by a simulated quadruped model with a CPG incorporating vestibular modulation

Article *in* Biological Cybernetics · October 2013

DOI: 10.1007/s00422-013-0572-4 · Source: PubMed

CITATIONS
17

READS
274

3 authors, including:

Yasuhiro Fukuoka
Ibaraki University
71 PUBLICATIONS **1,624** CITATIONS

SEE PROFILE

Yasushi Habu
Ibaraki University
5 PUBLICATIONS **47** CITATIONS

SEE PROFILE

Analysis of the Gait Generation Principle by a Simulated Quadruped Model with a CPG Incorporating Vestibular Modulation

Yasuhiro Fukuoka[1], Yasushi Habu[2] and Takahiro Fukui[3]

This study aims to understand the principles of gait generation in a quadrupedal model. It is difficult to determine the essence of gait generation simply by observation of the movement of complicated animals composed of brains, nerves, muscles, etc. Therefore, we build a planar quadruped model with simplified nervous system and mechanisms, in order to observe its gaits under simulation. The model is equipped with a mathematical Central Pattern Generator (CPG), consisting of four coupled neural oscillators, basically producing a trot pattern. The model also contains sensory feedback to the CPG, measuring the body tilt (vestibular modulation). This spontaneously gives rise to an unprogrammed lateral walk at low speeds, a transverse gallop while running, in addition to trotting at a medium speed. This is because the body oscillation exhibits a double peak per leg frequency at low speeds, no peak (little oscillation) at medium speeds, and a single peak while running. The body oscillation autonomously adjusts the phase differences between the neural oscillators via the feedback. We assume that the oscillations of the four legs produced by the CPG and the body oscillation varying according to the current speed are synchronized along with the varied phase differences to keep balance during locomotion through postural adaptation via the vestibular modulation, resulting in each gait. We succeeded in determining a single simple principle that accounts for gait transition from walking to trotting to galloping, even without brain control, complicated leg mechanisms, or a flexible trunk.

Keywords: Simulation study, Quadrupedal locomotion, Gait generation, Central pattern generator, and Vestibular modulation

Introduction

The gait transition of a quadruped according to its speed is well known [Hildebrand, 1965]. Alexander [Alexander, 1989] reported that animals tend to choose gaits (e.g., walking, trotting, and galloping) that optimize several criteria (maximum speed, endurance, energy cost, etc.). Biewener [Biewener, 1990] reported that an alteration in bone strain characterizes the trot-gallop transition in mammals. A redistribution of the skeletal load caused by a change in muscular recruitment is also an indicator of a gait transition [Farley and Taylor, 1991]. It was reported in the field of synergetic theory that gait changes take the form of non-equilibrium phase transitions [Schöner et al., 1990]. Hoyt and Taylor [Hoyt and Taylor, 1981] reported that horses change their gaits from walking to trotting to galloping as their speed increases to minimize their energy consumption. They also demonstrated that horses choose their speed to minimize their energy costs in each gait.

A vertebrate's spinal cord has a neural circuit called a Central Pattern Generator (CPG), which produces rhythmic patterns in its movements [Stent et al., 1978, Grillner, 1981, Pearson, 1985, Cohen, 1987, Bal et al., 1988]. The rhythms of the leg movements in quadrupedal locomotion are produced by this CPG [Brown, 1911, Shik et al., 1966, Grillner, 1981]. Shik et al. [Shik et al., 1966] demonstrated that mesencephalic cats on a treadmill exhibited a walking locomotion when an area of their midbrains to the CPG was electrically stimulated. In addition, they could switch from walking to trotting to galloping if either the strength of the stimulation or the speed of the treadmill was increased. A number of studies have been performed, based on these findings, to mathematically analyze the gait transition mechanism by utilizing a mathematical model of the CPG. This will be investigated further in the following section.

However, it is still uncertain how the order in which an animal moves its four legs in each gait is established. This order forms the generation principle of each gait. Our goal is developing a biomimetic quadruped robot that can locomote as a real animal. We first should know the gait generation principle of quasi-quadrupedal locomotion. Therefore, we have conducted computer simulations of the locomotion of a simple planar quadruped model with a simple CPG model incorporating vestibular modulation, which was constrained to the sagittal plane. As a result, although the interlimb coordination in the CPG model was hard-wired to produce a trot, varying the speed spontaneously generated a lateral walk (a lateral sequence walk) at low speeds and a transverse gallop at high speeds. Based on the result, we hypothesize that the oscillations of the four legs produced by the

[1]Yasuhiro Fukuoka,
Department of Intelligent Engineering, College of Engineering, Ibaraki University, 4-12-1 Nakanarusawa-cho, Hitachi-shi, Ibaraki 316-8511, Japan
e-mail: fukuoka@mx.ibaraki.ac.jp
TEL&FAX:+81-294-38-5203
[2]Yasushi Habu,
Graduate School of Science and Engineering, Ibaraki University, 4-12-1 Nakanarusawa-cho, Hitachi-shi, Ibaraki, 316-8511, Japan
[3]Takahiro Fukui,
Graduate School of Science and Engineering, Ibaraki University, 4-12-1 Nakanarusawa-cho, Hitachi-shi, Ibaraki, 316-8511, Japan

CPG and the body oscillation varying according to the current speed are synchronized along with the varied phase differences to keep balance during locomotion through postural adaptation via the vestibular modulation, resulting in each gait. We also use these results to discuss the generation principle of each gait.

Materials and Methods

Dynamical modeling approaches to gait analysis

In recent years, attempts have been made to relate a dynamical phenomenon to an animal by using a simulated model or a robot [Alexander, 2003, Miller et al., 2012] in order to elucidate the principle of the phenomenon.

As we mentioned earlier, the existence of a CPG discovered in biology was used by some researchers to construct a variety of CPG models. Nonlinear oscillators that govern each leg movement were coupled together, which allowed their models to reproduce the gait patterns observed on a quadruped [Willis, 1980, Stafford and Barnwell, 1985, Schöner et al., 1990, Yuasa and Ito, 1990, Collins and Richmond, 1994]. In quadrupeds, the need to modify limb coordination for walking, trotting, and galloping requires different sets of coordinating neurons [Grillner, 1985]. Modifications of the network parameters of a CPG (such as coupling strengths) allow switching between different gaits [Golubitsky et al., 1999]. Based on these findings, many studies built neural systems that modified parameters to govern interlimb coordination to produce typical gaits [Willis, 1980, Stafford and Barnwell, 1985, Matsuoka, 1987, Schöner et al., 1990, Yuasa and Ito, 1990, Buchli and Ijspeert, 2004]. Yuasa and Ito [Yuasa and Ito, 1990] were able to mimic the gait changing behavior observed as animals vary speed, using their quadruped model. In comparison, Collins and Richmond [Collins and Richmond, 1994] demonstrated that a hard-wired CPG model, where the network maintains an invariant coupling architecture, could produce walking, trotting and bounding behavior, by varying a driving signal to the CPG or the internal parameters of the individual oscillators.

Moreover, many researchers have begun to apply a CPG model to a quadruped model in either a simulation [Ito et al., 1998, Aoi et al., 2011, Harischandra et al., 2011] or a physical robot [Billard and Ijspeert, 2000, Tsujita et al., 2001, Fukuoka et al., 2003, Rutishauser et al., 2008, Tsujita et al., 2008, Santos and Matos, 2011, Owaki et al., 2012], allowing it to walk with a few typical gaits (walking, pacing, trotting, etc.), while taking into account the influence of the body as well as the CPG itself on the gait generation. Several of these researchers [Tsujita et al., 2001, Fukuoka et al., 2003, Aoi et al., 2011, Harischandra et al., 2011, Owaki et al., 2012] have aimed to investigate gait generation and/or the transition principle, and have demonstrated a quadruped model in simulation and/or a physical robot that can spontaneously generate typical walking gaits without explicitly handling phase differences between oscillators to produce each gait pattern. Sensory feedback from tactile or force sensors on the feet [Tsujita et al., 2001, Aoi et al., 2011, Owaki et al., 2012] and from a body inclinometer [Fukuoka et al., 2003] are returned to the CPG. A movable trunk mechanism was used [Aoi et al., 2011, Harischandra et al., 2011, Owaki et al., 2012]. It was discovered that the sensory feedback and the movable trunk mechanism have important roles in the generation of the walking gaits. Similarly, Schmiedeler and Waldron [Schmiedeler and Waldron, 1999] used a simulation model without a CPG to suggest that foot loading by thrust is related to spontaneous gait transition between galloping and bounding. Nakatani et al. [Nakatani et al., 2009] also demonstrated the effect of a passively movable trunk mechanism on the spontaneous gait generation of walking and trotting, by natural walking of a passive quadruped walker down a slope, without actuators or controls.

Based on these studies, we believe that gaits are generated by dynamical interaction between its nervous system and its body dynamics during locomotion. Several of the studies [Schmiedeler and Waldron, 1999, Tsujita et al., 2001, Fukuoka et al., 2003, Nakatani et al., 2009, Aoi et al., 2011, Harischandra et al., 2011, Owaki et al., 2012] demonstrated spontaneous gait generation and pointed out the importance of each of the elements that cause it. However, they omitted to explain how each gait is specifically generated by these elements. Moreover, there is no published model where both walking (walking, trotting, pacing, etc.) and running (galloping, bounding, etc.) are spontaneously generated through a single consistent logic. In the field of biomechanical engineering, a gait is called a symmetrical gait when the footfalls of the two feet of the fore and hind pairs of legs are evenly spaced in time. In an asymmetrical gait, at least one of the two pairs of limbs do not satisfy this property [Hildebrand, 1965]. It may be difficult to model the underlying mechanisms for walking (walking, trotting, pacing, etc.) and running (galloping, bounding, etc.) gaits using an identical principle, since the gaits appear to be symmetrical and asymmetrical, respectively [Maes et al., 2008].

A simulated quadruped model

In this study, we developed a computational quadruped model, simulated as shown in Fig. 1. We used a dynamic robot simulator called "Webots" [Michel, 2004]. Webots is regarded as a reliable simulator, and has been used in a number of recent locomotion studies [Tellez et al, 2006, Maufroya et al., 2008, Maufroya et al., 2010, Hauser et al., 2011, Santos and Matos, 2011].

We decided to use a simplified model, consisting of a linear elastic leg with one degree of freedom based on a Spring-Loaded Inverted Pendulum (SLIP) model [Cavagna et al., 1977, McMahon 1985]. In a variety

of animals, the locomotion of the whole body, including the legs, can be simplified using a SLIP model, which is a simple single massless spring with a point-mass attached above it [Blickhan and Full, 1993]. Although the SLIP model is simple, its dynamical features are very similar to those of an animal's locomotion. For example, the stance-phase patterns of a Centre of Mass (COM) trajectory in a SLIP model, vertical and fore-aft ground forces, and mechanical energy, are very similar to those observed in walking [Geyer et al., 2006] and running [Blickhan and Full, 1993, Koditschek et al. 2004] animals. Based on this observation, several multi-legged robots with linear legs have achieved stable locomotion [Raibert 1986, Lasa and Buehler, 2001, Cham et al., 2004, Poulakakis et al., 2006]. The linear legs of our quadruped model can work in the stance phase as the passive linear spring of the SLIP model and actively shorten in the swing phase. The tip of each leg is equipped with a small arched foot whose center of curvature is the hip joint. An active rotary hip joint is attached to each leg via a rigid body. Our quadruped model has eight joints in total; i.e., a rotary hip joint and a linear joint in each leg. The model was placed between two side walls without friction and constrained to sagittal motion to avoid tumbling sideways. We investigated the simple dynamics of gait generation that appear in the planar locomotion.

Trot gait production by a CPG model

A variety of CPG models for locomotion have been proposed [Willis, 1980, Cohen et al., 1982, Stafford and Barnwell, 1985, Matsuoka, 1987, Bay and Hemami, 1987, Yuasa and Ito, 1990, Schöner et al., 1990, Ekeberg et al., 1991, Collins and Richmond, 1994, Rybak et al., 2006]. Since our goal is to develop a biomimetic quadruped robot, we have adopted Matsuoka's neural oscillator model [Matsuoka, 1985, Matsuoka, 1987], which is a simple model with a smaller number of components than other realistic models based on the current literature of neuroscience that takes into account chemical interaction in cells, ionic currents, spike generation, etc. [Ekeberg et al., 1991, Rybak et al., 2006]. Matsuoka's model can mathematically achieve the basic ability of the CPG to produce locomotor activity while synchronizing multiple oscillations (e.g., oscillations of four legs, body oscillations) and is used for many simulation models and physical robots as a practical CPG model to reproduce rhythmic motions (e.g., monopod hopping [Pelc et al., 2008], biped walking [Taga, 1995a, Taga, 1995b, Hase and Yamazaki, 1988, Matsubara et al., 2006], quadruped walking [Fukuoka et al., 2003] and rhythmic arm movement [Miyakoshi et al., 1994, Williamson, 1998, Kotosaka and Schaal, 2000]).

A CPG model composed of four coupled neural oscillators prepared for our quadruped model is shown in Fig. 2 (the corresponding equations are in the Appendix at the end of the text). An individual leg is driven by both an extensor neuron and a flexor neuron. The output from each neuron inhibits other neurons via weights α, β and γ. The weights α, β and γ represent coefficients of connections in each leg between contralateral neurons, ipsilateral neurons, and extensor and flexor neurons, respectively. The four legs consist of lateral and sagittal symmetrical connections due to the mutual inhibitory connections through α and β. The extensor and flexor become an antagonistic muscle because of the mutual inhibitory connection, γ. The output of each neural oscillator from Fig. 2 is shown in Fig. 3. When the output is positive, the flexor neuron is excited, and when the output is negative, the extensor neuron is excited. A trot is observed, i.e., the outputs of the left foreleg and right hindleg are in phase and those of the right foreleg and left hindleg are also in phase, yet the two pairs together are out of phase.

Locomotion generation and control with the quadruped model

In this section, we detail a method that allows the quadruped model shown in Fig. 1 to move by means of the CPG model described in the previous section. Each leg is driven by a rhythm generator composed of the neural oscillator and a leg controller, as depicted in Fig. 4.

We will first explain the rhythm generator. The neural oscillator outputs the signal as shown in Fig. 3. This is only used to switch between the stance or swing phases. Specifically, if the flexor neuron is excited (the output is positive), the phase is "swing"; otherwise the phase is "stance" (i.e., when the output is zero, the phase is also regarded as the stance). The phase signs are then rhythmically transmitted to the leg controller.

The leg controller allows each leg to be controlled in each leg phase from the rhythm generator (the equations are given in the Appendix). Two simple motions should be possible on each leg. Specifically, the leg should be able to swing forward to prevent tripping in the swing phase, while the body should be supported during the stance phase. As shown in Fig. 4, in the swing phase, the linear leg is shortened toward a target length ($l_{d \cdot sw}$) and is swung forward to a target angle ($\theta_{d \cdot sw}$). In the stance phase, the linear leg is extended toward a target length ($l_{d \cdot st}$) and is swung backward to a target angle ($\theta_{d \cdot st}$). This allows it to thrust from the ground. When the linear leg touches the ground while it is extended to $l_{d \cdot st}$, it will behave like a compression spring whose free length is $l_{d \cdot st}$. Therefore, it will work as a linear elastic leg, as mentioned earlier in the SLIP model.

It is important to allow the oscillations of the oscillator and the body to synchronize through sensory feedback [Grillner, 1981, Andersson and Grillner, 1983, Ekeberg, 1993, Cohen and Boothe, 1999, Tytell and Cohen, 2008].

Specifically, proprioceptive sensory feedback has a strong impact [Grillner, 1981, Lam and Pearson, 2002, Frigon and Gossard, 2009]. Taga [Taga, 1995a, Taga, 1995b] achieved bipedal locomotion in a simulation where the oscillations of Matsuoka's oscillators and legs were allowed to

synchronize through the feedback of leg muscle lengths to the oscillators. This was also used for our quadruped robot "Tekken" [Fukuoka et al., 2003], which achieved spontaneous gait generation from a walk to a trot. We also applied this feedback to our quadruped model in this paper. Specifically, as depicted in Fig. 5, the lengths of the extensor and flexor of each hip joint are calculated from the joint angle. The lengths are multiplied by a weight, k_1, and input to the extensor and flexor neurons, respectively (the full equations are given in the Appendix). Thus, for example, if the extensor stretches, the extensor neuron is excited and the flexor neuron is inhibited.

Moreover, to synchronize the neural oscillation with the body oscillation, we utilize vestibular modulation activated according to vestibular information. This vestibular information is the original sensory feedback from our quadruped model. This approach was also used in our robot "Tekken" [Fukuoka et al., 2003]. The vestibular system acts to maintain balance and posture in an animal. For example, during whole body nose up tilts, there is an activation of extensors in both hindlimbs and activation of flexors in both forelimbs; the reverse activation is seen during nose-down tilts. This is called the vestibulospinal reflexes [Roberts, 1967]. This vestibular modulation was utilized for the pitching motion of our quadruped model in the sagittal plane. Specifically, as shown in Fig. 5, the body inclination around the pitch axis, which is positive while tilting forward, is multiplied by the weight k_2, and the extensor/flexor neurons are excited/inhibited (see the Appendix for the full equations). For example, while tilting forward, the extensor activity of the forelegs and the flexor activity of the hindlegs are increased, while conversely the flexor activity of the forelegs and the extensor activity of the hindlegs are decreased. The posture is therefore controlled. The weights k_1 and k_2 are constant.

The quadruped model with the above system, where all the parameters in the rhythm generator and the leg controller are constant, is capable of walking or running at a constant speed. To change the speed, we only modify the following speed control parameters to govern each leg's trajectory and walking cycle duration.

For example, to the increase the speed, we implement the following changes:

(a) A tonic descending signal with a constant rate input to every oscillator (denoted by s in the Appendix) is increased.

(b) The walking cyclic duration is shortened by decreasing the parameter governing the cycle of each oscillator (T_r in the Appendix).

(c) The desired hip joint angle in the stance phase, $\theta_{d\cdot st}$ (Fig. 4), is decreased to swing each support leg further backwards, and its control gain ($K^{\tau}_{pi\cdot st}$ in the Appendix) is increased to quickly reach the desired angle.

(d) To increase each leg's stiffness according to speed, a gain ($K^{F}_{pi\cdot st}$ in the Appendix) to govern the modulus of elasticity of each linear knee joint in the stance phase is increased.

(e) To prevent the tip of the leg from catching the ground in the swing phase, the desired length of the linear knee joint, $l_{d\cdot sw}$ (Fig. 4), is decreased, and its control gain ($K^{F}_{pi\cdot sw}$ in the Appendix) is increased to quickly shorten each leg.

It should be noted that the parameters to directly dominate the relation among legs (i.e., the connection weights α and β between the neural oscillators, and the parameter of the vestibular modulation, k_2) are always fixed, even while the speed is changing.

Results

In this section, we show our simulation results for walking and running, where the planar quadruped models with and without the vestibular modulation are used. We first set the speed control parameters described in Steps (a) to (e) of the previous section so that the quadruped model without vestibular modulation ($k_2 = 0$ in Fig. 5) can proceed safely with constant acceleration and deceleration. Next, the quadruped model with vestibular modulation ($k_2 > 0$) uses the same parameters as the model without, with the exception of k_2. We observed the gaits generated by the two models. Their locomotion movies can be seen at http://fukuoka.ise.ibaraki.ac.jp/.

When the diagonal pairs of legs move in phase and the pairs move out of phase with each other, this gait is defined as a trot. In this paper, if the time difference between the two footfalls of either of the diagonal pairs becomes more than 5% of the walking cyclic duration, we consider that the gait has left the trot state. When the feet touch the ground in the order left fore, right hind, right fore, and left hind, we regard the gait as a lateral walk. When the feet touch the ground in the order left fore, right fore, left hind, and right hind, or in the order right fore, left fore, right hind, and left hind, we regard the gait as a transverse gallop.

Simulation of the quadruped model without vestibular modulation

We allowed the quadruped model without vestibular modulation ($k_2 = 0$ in Fig. 5) to proceed at an approximately constant acceleration (0.05 m/s^2) and deceleration (-0.05 m/s^2), as shown in Fig. 6. Simulation results when speeding up from 3 s to 23 s and slowing down from 45 s to 59 s, as shown in Fig. 6, are shown in Figs. 7 and 8, respectively. The simulation is in the file "Movie 1" in the above-mentioned web site. In Figs. 7 and 8, the top oscillations indicate the output of the neural oscillators: LF: left fore (blue); LH: left hind (red); RF: right fore (green); and RH: right hind (purple). The solid and dashed lines are used to show the fore and hind legs, respectively. The middle waves show the body inclination (positive while tilting forward). Thick line segments on a thin dashed line in the bottom show each leg's footfalls. It can be observed that the model was trotting all the

time in each speed, as in Fig. 3. The model ran with a flying trot for approximately 12 s to 48 s in Figs. 6, 7 and 8, since its duty factor decreased in relation to the speed.

Simulation of the quadruped model with vestibular modulation

We also designed a quadruped model with vestibular modulation where the value of k_2 for the previous quadruped model without vestibular modulation was only changed to a certain fixed value. All other values were kept identical. The same simulation was performed using the same speed control parameters. The simulation results during acceleration and deceleration are shown in Figs. 9 and 10, respectively. The simulation is shown in "Movie 2" in the above-mentioned web site. Although this model only varied by the value of k_2 from the previous model, gaits other than the trot can be seen in both Fig. 9 and Fig. 10. For example, we observe a lateral walk between 3.3 s to 9.3 s in Fig. 9, followed by a trot, and a transverse gallop after 20.2 s. The order of the neural oscillator outputs is seen to begin to transform to a transverse gallop from 19.6 s, yet the order of the footfalls has not completely changed to a transverse gallop for 19.6 s to 20.2 s because of temporal instability during the transition process. In Fig. 10, the gaits are seen to transition from a transverse gallop to a trot to a lateral walk, as the speed decreased. We can observe that the neural oscillator output is zero, noticeably at the low speeds in Fig. 10. We currently regard this period as the same as in the extensor neuron excitation (negative of the output) in our study as we mentioned before. Without any control in the zero period, the tip of the loose leg catches on the ground and the model falls forward. If the zero period is involved in the flexor neuron excitation, only the two-legged support period, such as trotting, appears at very low speeds (A in Fig. 10), resulting in it falling sideways in the 3D walking.

It can be observed in Figs. 9 and 10 that the lateral walk and the transverse gallop emerged at low and high speeds, where the body inclination was significant. This is because that the too long stance phase at low speeds and nonrestraint during the flight phase at high speeds give rise to significant body oscillation. Our quadruped model attempted to keep balance through vestibular modulation during the body oscillation; therefore, the phase differences among the four oscillators were adjusted, resulting in autonomous generation of the two gaits. When operating at a medium speed, where the stance phase is moderately short and the flight phase does not exist, the body oscillated only slightly, remaining stable (see 9.3 s to 19 s in Fig. 9 and 51 s to 53 s in Fig. 10). Therefore, the vestibular modulation did not work and the gait became a trot, which is inherently produced by the neural oscillator network. We theorize that each gait emerges as a result of the oscillations of the four legs produced by the CPG and the body oscillation varying according to speed. These oscillations are synchronized along with varied phase differences while keeping balance during locomotion by postural adaptation through the vestibular modulation, resulting in the gaits.

The speed of the simulation shown in Figs. 9 and 10 is shown in Fig. 11 by the black line. The speed of the simulation from Fig. 6 is also shown for comparison by the purple line. The speed of the model with vestibular modulation was very high during the transverse gallop, although its speed control parameters, described by Steps (a) to (e) in the section "Materials and Methods" earlier, were exactly the same as those of the model without vestibular modulation, which was seen to trot continuously. The body oscillation during the transverse gallop was greater than that observed during the lateral walk and the trot as seen in Figs. 9 and 10. Howell [Howell 1944] related the body inclination to speed, reporting that increasing the movement of the head, neck, and back is a feature of a gallop, which explains why a greater increase in speed is obtained for a gallop than for any other gait. Our simulation results seem consistent with this finding, limited to the movement of its back (a head and neck are omitted from our model). It can be seen by the black line in Fig. 11 that the speed transition between trotting and transverse galloping was abrupt, whereas the transition between lateral walking and trotting was seamless. The abrupt transition tendency seemed especially prominent during acceleration.

Gait generation for various vestibular modulation levels

We observed in the previous simulations that the vestibular modulation plays a significant role in the generation of the walk and gallop gaits. In this section, we investigate how the generated gaits vary according to the value of k_2 (the vestibular modulation level) in Fig. 5. In Fig. 12, the simulation results for the quadruped models with an arbitrary value for k_2 between 0 and 20 are shown. The same values for the speed control parameters as in the previous simulations were used. The X-, Y-, and Z-axes represent time, the vestibular modulation level k_2, and speed, respectively. We have marked the gaits on the figure, emerged in the simulations. The various gaits are separated by dots and four dashed lines based on the definition of each gait as described in this paper. We introduce a new definition of gait, called a "bound", if the phase difference between the two feet in both fore and hind pairs reduces to no more than 5% of the running cyclic duration and the phase difference between both pairs increases by over 45-55% of the running cyclic duration.

It can be seen that the data in Fig. 12 drops off above 30 s when k_2 is in the range 15-20. This suggests that the model did not keep up with the speed and fell over. The speed graphs shown in Fig. 6 and Fig. 11, for the models with and without vestibular modulation in the previous sections, correspond to the plots in the X-Z plane of $k_2 = 0$ and 9.3, respectively. For example, when $k_2 = 9.3$ in Fig. 12, the gait changed from a lateral walk to a trot to a transverse gallop to a trot to a lateral walk, as observed in Figs. 9 and 10. If k_2 is greater than or equal to 3, a lateral walk was

observed at a low speed. In addition, if k_2 has a value of 4 or above, a transverse gallop occurs at high speed. Moreover, when the vestibular modulation level is high (i.e., k_2 is between 18 and 20), a bound emerged at high speeds (more than approximately 1.2 m/s). This is due to the effect of the vestibular modulation on the neural oscillator, which was too strong in comparison to the interlimb coordination built by the couplings between the neural oscillators. For example, when the model tilts forward, the extension of both forelimbs and the flexion of both hindlimbs increases too strongly through the excessive vestibular modulation. Therefore, the gait transitioned to a bound, where the two feet of both the fore and hind pairs are almost in phase and the pairs are out of phase. At approximately 23 s, the gait changes from a trot to a transverse gallop to a bound as k_2 increases following the arrow α, in Fig. 12. When k_2 is in the range 18-20, the gaits varied from a trot to a transverse gallop to a bound according to speed, following the arrow β. Therefore, the transverse gallop appears to be a type of transition gait between trotting and bounding. Collins and Stewart [Collins and Stewart, 1993] also reported that the transverse gallop is a mixture of a trot and a bound.

Gait generation at various accelerations and decelerations

In this section, we investigate how gait generation depends on speed. The simulation will show if we can achieve the same gait transition in the locomotion of the quadruped model with vestibular modulation at different accelerations and decelerations.

The acceleration and deceleration in Fig. 6 were approximately $\pm 0.05 \mathrm{m/s^2}$, resulting in a trot in the quadruped model without vestibular modulation. We define these values as VAD (e.g., VAD was $\pm 0.05 \mathrm{m/s^2}$ for Fig. 6). Fig. 13 shows the plots for each speed when the quadruped model with vestibular modulation walked and ran using the speed control parameters to give the desired VAD. The other parameter values are identical to those in Figs. 9 and 10. In Fig. 13, VAD = ± 0.167 m/s^2 (A), ± 0.083 m/s^2 (B), ± 0.063 m/s^2 (C), ± 0.05 m/s^2 (D), ± 0.042 m/s^2 (E), ± 0.033 m/s^2 (F), ± 0.025 m/s^2 (G). The plot for D is equivalent to the black line in Fig. 11. It is seen that a lateral walk and a transverse gallop were generated for each speed variation. The location of each gait transition is marked by a $\circ$ in Fig. 13. It can be seen that all choices for VAD have the same tendency as observed in Fig. 11, where the speed transition between the lateral walk and the trot was seamless, whereas the speed transition between the trot and the transverse gallop was relatively abrupt. The transition between the trot and the transverse gallop seems abrupt, even for a small acceleration and deceleration, such as in the cases of F and G (particularly for the trot to transverse gallop). We propose that the two gaits will always transition abruptly between each other for any acceleration and deceleration since they are categorized as different types of gait (i.e., a trot is a symmetrical gait, while a gallop is an asymmetrical gait). It can be seen that the speed at the moment of each gait transition is fairly constant: for the lateral walk to trot transition, it is approximately 0.38 m/s; for the trot to transverse gallop, it is 1.02 m/s; the transverse gallop to trot is 0.4 m/s; and the trot to lateral walk is 0.25 m/s. The speed of each gait transition is independent of the acceleration or deceleration, although they are adjusted by the change of the several speed control parameters, and may inherently be determined by the body dynamics of the quadruped model. To investigate the effect of the mechanical design on the speed of each gait transition, we allowed the quadruped model with a different weight of the rigid trunk to perform the same simulation as in Fig. 13, where all the same control parameters were used. As a result, the speed of each gait transition was nearly constant independently of the acceleration or deceleration similar to Fig. 13. However, the transition speed between the trot and the transverse gallop became obviously small as the trunk weight increased, while that between the walk and the trot was approximately invariant. Specifically, when we changed the weight from the default 7kg to 10kg or 16kg, the transition speed from the trot to the transverse gallop was 0.9 m/s or 0.47 m/s, respectively (1.02 m/s by 7kg); from the transverse gallop to the trot, 0.32 m/s or 0.24 m/s (0.4 m/s by 7kg). This is consistent with the findings of Farley and Taylor [Farley and Taylor, 1991], where when horses carried weights, they switched from a trot to a gallop at a lower speed.

Discussion

We demonstrated in the Results section that a transverse gallop and a lateral walk are spontaneously generated from a trot, which is inherently produced by the neural oscillators' network, as an effect of the vestibular modulation. This result supported our hypothesis that each gait emerges as a result of the oscillations of the four legs produced by the CPG and the body oscillation varying according to speed, and that these oscillations are synchronized along with varied phase differences while keeping balance during locomotion by postural adaptation through the vestibular modulation, resulting in the gaits. In this section, we will discuss how the vestibular information specifically affects the neural oscillators for each gait's generation and a correlation between posture control and gait generation.

Generation of a transverse gallop from a trot

In Fig. 14, the neural oscillator outputs and the body inclination during the gait transition from a trot to a transverse gallop at approximately 19 s to 20 s from Fig. 9 is shown. The flying trot, which has suspended phases, appeared when the model accelerated during a walking trot. In the flight phase, the body has begun to gradually oscillate, as shown in Fig. 14. This body inclination activates the vestibular modulation and gives rise to phase differences between the

oscillators. The arrows in the figure are used to represent excitation or inhibition of the flexor/extensor neuron in each leg's neural oscillator. This excitation/inhibition was caused by the feedback of the body inclination to the neural oscillator.

For example, the period T_1 in Fig. 14 shows the state when the body inclined slightly forward. For the neural oscillator outputs of the forelegs, the excited extensor neuron of the left foreleg (blue line) was more excited by being pulled down as directed by the blue arrows, and the excited flexor neuron of the right foreleg (green line) was inhibited by being pulled down as directed by the green arrows. For the neural oscillator outputs of the hindlegs, the excited flexor neuron of the left hindleg (red line) was more excited by being pulled up as directed by the red arrows, and the excited extensor neuron (purple line) was inhibited being pulled up as directed by the purple arrows. In short, when tilting forward, the oscillator outputs of the forelegs are pulled down and those of the hindlegs are pulled up. Conversely, when tilting backward as in the period marked by T_2, the oscillator outputs of the forelegs were pulled up and those of the hindlegs were pulled down.

Therefore, as the body inclination increased, the phases of the neural oscillator outputs of the two right legs advanced while those of the two left legs are delayed. In other words, the outputs from the RF and RH have shifted to the left, while the outputs from the LF and LH have shifted to the right. Therefore, the phase between the two feet in the fore and hind pairs came closer. As a result, the two feet in both the fore and hind pairs became unevenly spaced in time. This indicates that the gait switched from a trot (symmetrical gait) to an asymmetrical gait. Specifically, the oscillator outputs transitioned to the order LF, RF, LH, and RH, which exhibits a transverse gallop (asymmetrical gait).

Generation of a lateral walk from a trot

In Fig. 15, the neural oscillator outputs and body inclination during the gait transition from a trot to a lateral walk at approximately 53 s to 55 s from Fig. 10 is shown. The walking cyclic duration (specifically, the period of the stance phase) increases as the speed decreases; this results in body oscillation. This body inclination has activated the vestibular modulation and given rise to phase differences between the oscillators. The arrows represent excitation or inhibition of the flexor/extensor neuron provoked by the body inclination as in the previous section. Therefore, it is observed in Fig. 15 that the phases of both forelegs (LF and RF) were gradually advancing from those of both hindlegs (LH and RH) and the phase difference has increased. In other words, the outputs of the LF and RF have shifted to the left, while the outputs of the LH and RH have shifted to the right as the body oscillation increased. However, the two feet in both the fore and hind pairs have remained evenly spaced in time (a symmetrical gait) from 53 s onwards while trotting. The oscillator outputs finally transitioned to the order LF, RH, RF, and LH, which is called a lateral walk (a symmetrical gait).

Variation in the gait generation principle between a lateral walk and a transverse gallop

The transverse gallop and the lateral walk were generated in a similar manner due to the body inclination around the pitch axis. Nevertheless, the two gaits that emerged were distinct. This is because the ratio between the body's frequency and each leg's frequency has naturally become equal to 1:1 in the high-speed (running) trotting, while the ratio tends to be 2:1 in the low-speed trotting, as shown in Fig. 7. It is reported in terms of a biped locomotion that the ratio tends to be 1:1 for running, while 2:1 for walking [Geyer et al., 2006]. If the two legs of each diagonal pair in trotting are regarded a single leg, the trot resembles a biped locomotion. We have considered that the difference of the body's frequency, according to the speed, gives rise to the two gaits. The different body frequencies tend to remain even after the gait transitions (Figs. 14 and 15). This is consistent with Muybridge's findings [Muybridge 1957], where movements of the head and neck (a body) exhibit a single peak per stride for a gallop, while double peaks were observed for a walk. We conclude that the body dynamics varying according to the speed synchronized with the hard-wired CPG, and that the gaits of the transverse gallop and the lateral walk were therefore generated from a trot.

Correlation between posture control and gait generation

Our quadruped robot "Tekken" [Fukuoka et al., 2003], which aimed to safely walk over irregular terrain, used the vestibular modulation described in this paper for its rolling motion, not its pitching motion; therefore, a lateral walk was spontaneously generated. In the quadruped model of this paper constrained in the sagittal plane, the transverse gallop emerged in addition to the lateral walk through the vestibular modulation for its pitching motion. As a result, we consider that regimes of posture control and gait generation are similar. Since body oscillations that occur while walking over irregular terrain are irregular disturbances, phase differences between four legs are irregularly (but appropriately) adjusted through the vestibular modulation, and the posture is controlled. On the other hand, since body oscillations that occur in the slow walking and running on flat terrain are regular disturbances, regular phase differences between four legs are generated through the vestibular modulation, a so-called lateral walk and transverse gallop.

Acknowledgements

The authors declare no competing financial interests. This work is supported by Japan Society for the Promotion of Science (Grant-in-Aid for Young Scientists (B)) and Ibaraki University (Life Support

Project). We would like to thank Kazuyoshi Mori, Naoji Shiroma and Kosuke Inoue for their valuable comments and advice.

References

[Alexander, 1989] Alexander, R. M. (1989). Optimization and gaits in the locomotion of vertebrates. *Physiological reviews*. **69**, 1199-1227.

[Alexander, 2003] Alexander, R. M. (2003). Modelling approaches in biomechanics. *Philosophical Transactions of the Royal Society B*. **358**, 1429-1435.

[Andersson and Grillner, 1983] Andersson, O. and Grillner, S. (1983). Peripheral control of the cat's step cycle. II Entrainment of the central pattern generators for locomotion by sinusoidal hip movements during fictive locomotion. *Acta. Physiol. Scand*. **118**, 229-239.

[Aoi et al., 2011] Aoi, S., Yamashita, T. and Tsuchiya, K. (2001). Hysteresis in the gait transition of a quadruped investigated using simple body mechanical and oscillator network models. *Physical Review E*. **83**, 061909-1-12.

[Bal et al., 1988] Bal, T., Nagy, F and Moulins, M. (1988) The pyloric central pattern generator in Crustacea: a set of conditional neuronal oscillators *Journal of Comparative Physiology A*. **163**, 715-727.

[Bay and Hemami, 1987] Bay, J. S. and Hemami, H. (1987). Modeling of a neural pattern generator with coupled nonlinear oscillators. *IEEE Trans. Biomed. Eng.*. **34**, 297-306.

[Biewener, 1990] Biewener, A. A. (1990). Biomechanics of mammalian terrestrial locomotion. *Science*. **250**, 1097-1103.

[Billard and Ijspeert, 2000] Billard, A. and Ijspeert, A. J. (2000). Biologically inspired neural controllers for motor control in a quadruped robot. *Proc. of the IEEE-INNS-ENNS Int. Joint Conf. on Neural Networks 2000*. **6**, 637-641.

[Blickhan and Full, 1993] Blickhan, R. and Full, R. J. (1993). Similarity in multilegged locomotion: Bouncing like a monopode. *J. of Comparative Physiology A*. **173**, 509-517.

[Brown, 1911] Brown, T. G. (1911). The Intrinsic Factors in the Act of Progression in the Mammal *Proc. of Roy Soc of London. Ser B*. **84**, 308-319.

[Buchli and Ijspeert, 2004] Buchli, J. and Ijspeert, A. J. (2004). Distributed Central Pattern Generator Model for Robotics Application Based on Phase Sensitivity Analysis. *Proc. of the First International Workshop on the Biologically Inspired Approaches to Advanced Information Technology 2004*. **3141**, 333-349.

[Cavagna et al., 1977] Cavagna, G. A., Heglund, N. C. and Taylor, C. R. (1977). Mechanical work in terrestrial locomotion: two basic mechanisms for minimizing energy expenditure. *American J. of Physiology*. **233**, R243-R261.

[Cham et al., 2004] Cham, J. G., Karpick, J. and Cutkosky, M. R. (2004). Stride Period Adaptation for a Biomimetic Running Hexapod. *International Journal of Robotics Research*. **23**, 141-153.

[Cohen et al., 1982] Cohen, A. H., Holmes, P. J. and Rand, R. H. (1982). The nature of the coupling between segmental oscillators of the lamprey spinal generator for locomotion: a mathematical model. *J. of Mathematical Biology*. **13**, 345-69.

[Cohen, 1987] Cohen, A. H. (1987). Effects of oscillator frequency on phase-locking in the lamprey central pattern generator. *Journal of Neuroscience Methods*. **21**, 113-125.

[Cohen and Boothe, 1999] Cohen, A. H. and Boothe, D. L. (1999). Sensorimotor Interactions During Locomotion: Principles Derived from Biological Systems. *Autonomous Robotics*. **7**, 239-245.

[Collins and Stewart, 1993] Collins, J. J. and Stewart, I. N. (1993). Coupled nonlinear oscillators and the symmetries of animal gaits. *J. of Nonlinear Science*. **3**, 349-392.

[Collins and Richmond, 1994] Collins, J. J. and Richmond, S. A. (1994). Hard-wired central pattern generators for quadrupedal locomotion. *Biological Cybernetics*. **71**, 375-385.

[Ekeberg et al., 1991] Ekeberg, Ö., Wallén, P., Lansner, A., Tråvén, H., Brodin, L. and Grillner, S. (1991). A computer based model for realistic simulations of neural networks. I. The single neuron and synaptic interaction *Biological Cybernetics*. **65**, 81-90.

[Ekeberg, 1993] Ekeberg, Ö. (1993). A combined neuronal and mechanical model of fish swimming *Biological Cybernetics*. **69**, 363-374.

[Farley and Taylor, 1991] Farley, C. T. and Taylor, C. R. (1991). A mechanical trigger for the trot-gallop transition in horses. *Science*. **253**, 306-308.

[Frigon and Gossard, 2009] Frigon, A. and Gossard, J. P. (2009). Asymmetric control of cycle period by the spinal locomotor rhythm generator in the adult cat. *J. of Physiology*. **587**, 4617-4628.

[Fukuoka et al., 2003] Fukuoka, Y., Kimura, H. and Cohen, A. H. (2003). Adaptive Dynamic Walking of a Quadruped Robot on Irregular Terrain based on Biological Concepts. *Int. J of Robotics Research*. **22**, 187-202.

[Geyer et al., 2006] Geyer, H., Seyfarth, A. and Blickhan, R. (2006). Compliant leg behaviour explains basic dynamics of walking and running. *Proc. of the Royal Society B*. **273**, 2861-2867.

[Golubitsky et al., 1999] Golubitsky, M., Stewart, I., Buono, P. L. and Collins, J. J. (1999). Symmetry in locomotor central pattern generators and animal gaits. *Nature*. **401**, 693-695.

[Grillner, 1981] Grillner, S. (1981). Control of Locomotion in Bipeds, Tetrapods, and Fish. *In Handbook of Physiology. The Nervous System, Motor Control*. **2**, 1179-1236.

[Grillner, 1985] Grillner, S. (1985). Neurobiological bases of rhythmic motor acts in vertebrates. *Science*. **228**, 143-149.

[Harischandra et al., 2011] Harischandra, N., Knuesel, J., Kozlov, A., Bicanski, A., Cabelguen, J. M., Ijspeert, A. and Ekeberg, Ö. (2011). Sensory feedback plays a significant role in generating walking gait and in gait transition in salamanders : a simulation study. *Frontiers in Neurorobotics*. **5**, 1-13.

[Hase and Yamazaki, 1988] Hase, K. and Yamazaki, N. (1988). Computational evolution of human bipedal walking by a neuro-musculo-skeletal model. *Artificial Life and Robotics* **3**, 133-138.

[Hauser et al., 2011] Hauser, H., Neumann, G., Ijspeert, A. J. and Maass, W. (2011). Biologically inspired kinematic synergies enable linear balance control of a humanoid robot. *Biological Cybernetics*. **104**, 235-249.

[Hildebrand, 1965] Hildebrand, M. (1965). Symmetrical Gaits of Horses. *Science*. **150**, 701-708.

[Howell 1944] Howell, A. B. (1944). Speed in animals; their specialization for running and leaping. *New York, Hafner Pub. Co.*

[Hoyt and Taylor, 1981] Hoyt, D. F. and Taylor, C. R. (1981). Gait and the energetics of locomotion in horses. *Nature*. **292**, 239-240.

[Ito et al., 1998] Ito, S., Yuasa, H., Luo, Z. W., Ito, M. and Yanagihara, D. (1998). A mathematical model of adaptive behavior in quadruped locomotion. *Biological Cybernetics*. **78**, 337-347.

[Jayes and Alexander, 1978] Jayes, A. S. and Alexander, R. M. (1978). Mechanics of locomotion of dogs (Canis familiaris) and sheep (Ovis aries). *Journal of Zoology*. **185**, 289-308.

[Koditschek et al. 2004] Koditschek, D. E., Full, R. J. and Buehler, M. (2004). Mechanical aspects of legged locomotion control. *Arthropod Structure & Development*. **33**, 251-272.

[Kotosaka and Schaal, 2000] Kotosaka, S. and Schaal, S. (2000). Synchronized robot drumming by neural oscillator. *Proc. of the Int. Symp. on Adaptive Motion of Animals and Machines*.

[Kuramoto, 1975] Kuramoto, Y. (1975). Self-entrainment of a population of coupled non-linear oscillators. *Int. Symp. on Mathematical Problems in Theoretical Physics Lecture Notes in Physics*. **39**, 420-422.

[Lam and Pearson, 2002] Lam, T. and Pearson, K. G. (2002). The role of proprioceptive feedback in the regulation and adaptation of locomotor activity. *Advances in Experimental Medicine and Biology*. **508**, 343-55.

[Lasa and Buehler, 2001] Lasa, M. and Buehler, M. (2001). Dynamic compliant quadruped walking. *Proc. of the IEEE International Conference on Robotics and Automation 2001*. **3**, 3153-3158.

[Maes et al., 2008] Maes, L. D., Herbin, M., Hackert, R., Bels, V. L. and Abourachid, A. (2008). Steady locomotion in dogs: temporal and associated spatial coordination patterns and the effect of speed. *J. of Experimental Biology*. **211**, 138-149.

[Matsubara et al., 2006] Matsubara, T., Morimoto, J., Nakanishi, J. Sato, M. and Doya, K. (2006). Learning CPG-based biped locomotion with a policy gradient method. *Robotics and Autonomous Systems*. 54, 911-920.

[Matsuoka, 1985] Matsuoka, K. (1985). Sustained Oscillations Generated by Mutually Inhibiting Neurons with Adaptation. *Biological Cybernetics*. **52**, 367-376.

[Matsuoka, 1987] Matsuoka, K. (1987). Mechanisms of Frequency and Pattern Control in the Neural Rhythm Generators. *Biological Cybernetics*. **56**, 345-353.

[Maufroya et al., 2008] Maufroya, C., Kimura, H. and Takase, K. (2008). Towards a general neural controller for quadrupedal locomotion. *Neural Networks*. **21**, 667-681.

[Maufroya et al., 2010] Maufroya, C., Kimura, H. and Takase, K. (2010). Integration of posture and rhythmic motion controls in quadrupedal dynamic walking using phase modulations based on leg loading/unloading. *Autonomous Robot*. **28**, 331-353.

[McMahon 1985] McMahon, T. A. (1985). The role of compliance in mammalian running gaits. *J Exp Biol*. **115**, 263-282.

[Michel, 2004] Michel, O. (2004). Cyberbotics Ltd. WebotsTM: Professional Mobile Robot Simulation. *Int. J. of Advanced Robotic Systems*. **1**, 2004.

[Miller et al., 2012] Miller, L. A., Goldman, D. I., Hedrick, T, L., Tytell, E. D., Wang, Z. J., Yen, J. and Alben, S. (2012). Using Computational and Mechanical Models to Study Animal Locomotion. *Integrative and Comparative Biology*. 1-23.

[Miyakoshi et al., 1994] Miyakoshi, S., Yamakita, M., Furuta, K. (1994). Juggling control using neural oscillators. *Proc. of the IEEE/RSJ Int. Conf. on Intelligent Robots and Systems*. 1186-1193.

[Muybridge 1957] Muybridge, E. (1957). Animals in Motion. *Dover Publications*.

[Nakatani et al., 2009] Nakatani, K., Sugimoto, Y. and Osuka, K. (2009). Demonstration and Analysis of Quadrupedal Passive Dynamic Walking. *Advanced Robotics*. **23**, 483-501.

[Owaki et al., 2012] Owaki, D., Morikawa, L. and Ishiguro, A. (2012). Gait Transition of Quadruped Robot without Interlimb Neural Connections. *Proc. of Dynamic Walking 2012*.

[Pearson, 1985] Pearson, K. G. (1985). Are there central pattern generators for walking and flight in insects? *In W. J. P. Barnes & M. H. Gladden (Eds.), Feedback and motor control in invertebrates and vertebrates*. 307-315.

[Pearson et al., 2006] Pearson, K. G., Ekeberg, Ö. and Büschges, A. (2006). Assessing sensory function in locomotor systems using neuro-mechanical simulations. *Trends in Neurosciences*. **29**, 625-631.

[Pelc et al., 2008] Pelc, E. H., Daley, M. A. and Ferris, D. P. (2008). Resonant hopping of a robot controlled by an artificial neural oscillator *Bioinsp. Biomim.*. **3**, 260-261.

[Poulakakis et al., 2006] Poulakakis, I., Papadopoulos, E. and Buehler, M. (2006). On the Stability of the Passive Dynamics of Quadrupedal Running with a Bounding Gait. *Int. J. of Robotics Research*. **25**, 669-687.

[Raibert 1986] Raibert, M. H. (1986). Legged robots that balance. *MIT Press*.

[Roberts, 1967] Roberts, T. D. M. (1967). Neurophysiology of Postural Mechanisms. *Butterworth*.

[Rutishauser et al., 2008] Rutishauser, S., Sproewitz, A., Righetti, L. and Ijspeert, A. J. (2008). Passive compliant quadruped robot using central pattern generators for locomotion control. *Proc. of the Int. Conf. on Biomedical Robotics and Biomechatronics*. 710-715.

[Rybak et al., 2006] Rybak, I. A., Shevtsova, N. A., Lafreniere-Roula, M. and McCrea, D. A. (2006). Modelling spinal circuitry involved in locomotor pattern generation: insights from deletions during fictive locomotion *J. of Physiology*. **577**, 617-639.

[Santos and Matos, 2011] Santos, C. P. and Matos, V. (2011). Gait transition and modulation in a quadruped robot: A brainstem-like modulation approach. *Robotics and Autonomous Systems*. **59**, 620-634.

[Schmiedeler and Waldron, 1999] Schmiedeler, J. P. and Waldron, K. J. (1999). The Mechanics of Quadrupedal Galloping and the Future of Legged Vehicles. *Int. J. of Robotic Research*. **18**, 1224-1234.

[Schöner et al., 1990] Schöner, G., Jiang, W. Y. and Kelso, J. A. S. (1990). A Synergetic Theory of Quadrupedal Gaits and Gait Transitions. *J of Theoretical Biology*. **142**, 359-391.

[Shik et al., 1966] Shik, M. L., Severin, F. V. and Orlovsky, G. N. (1966). Control of walking and running by means of electrical stimulation of the midbrain. *Biophysics*, **11**, 756-765.

[Stafford and Barnwell, 1985] Stafford, F. S. and Barnwell, G. M. (1985). Mathematical models of central pattern generators in locomotion: III. Interlimb model for the cat. *J. of Motor Behavior*. **17**, 60-76.

[Stent et al., 1978] Stent, G. S., Kristan, W. B. Jr, Friesen, W. O., Ort, C. A., Poon, M. and Calabrese, R. L. (1978). Neuronal Generation of the Leech Swimming Movement. *Science*. **200**, 1348-1357.

[Taga, 1995a] Taga, G. (1995). A model of the neuro-musculo-skeletal system for human locomotion. I. Emergence of basic gait. *Biological Cybernetics*. **73**, 97-111.

[Taga, 1995b] Taga, G. (1995). A model of the neuro-musculo-skeletal system for human locomotion. II. Real-time adaptability under various constraints. *Biological Cybernetics*. **73**, 113-121.

[Tellez et al, 2006] Tellez, L. H. R., Michel, O. and Ijspeert, A. (2006). Aibo and Webots: Simulation, wireless remote control and controller transfer. *Robotics and Autonomous Systems*. **54**, 472-485.

[Tsujita et al., 2001] Tsujita, K., Tsuchiya, K. and Onat, A. (2001). Adaptive gait pattern control of a quadruped locomotion robot. *Proc. of the 2001 IEEE/RSJ International Conference on Intelligent Robots and Systems 2001*. 2318-2325.

[Tsujita et al., 2008] Tsujita, K., Kobayashi, T., Inoura, T. and Masuda, T. (2008). Gait Transition by Tuning Muscle Tones using Pneumatic Actuators in Quadruped Locomotion. *Proc. of The 2006 IEEE/RSJ International Conference on Intelligent Robots and Systems*. 2453-2458.

[Tytell and Cohen, 2008] Tytell, E. D. and Cohen, A. H. (2008). Rostral versus caudal differences in mechanical entrainment of the lamprey central pattern generator for locomotion. *Journal of Neurophysiology* vol.99, pp.2408-2419.

[Williamson, 1998] Williamson, M. M. (1998). Neural control of rhythmic arm movements. *Neural Networks*. **11**, 1379-1394.

[Willis, 1980] Willis, J. B. (1980). On the interaction between spinal locomotor generators in quadrupeds. *Brain Research*. **2**, 171-204.

[Yuasa and Ito, 1990] Yuasa, H. and Ito, M. (1990). Coordination of many oscillators and generation of locomotory patterns. *Biological Cybernetics*. **63**, 177-184.

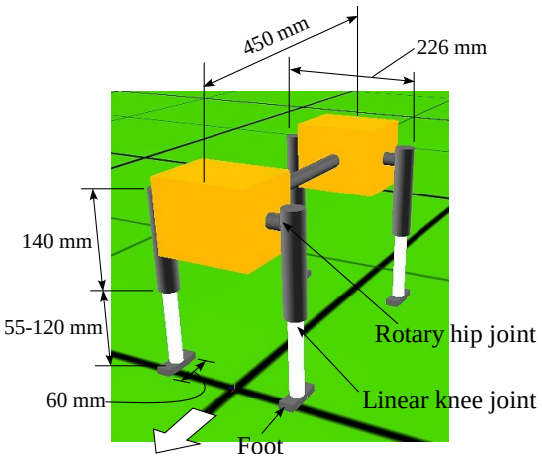

Figure 1: A simple quadruped model built in a dynamic simulator, which can be used to roughly mimic small animals. The model has eight joints; i.e., a rotary hip joint and a linear joint in each leg. The trunk is rigid. The model weighs 7.84 kg (210 g per leg, and 7 kg for the body). Its movement is constrained in the sagittal plane.

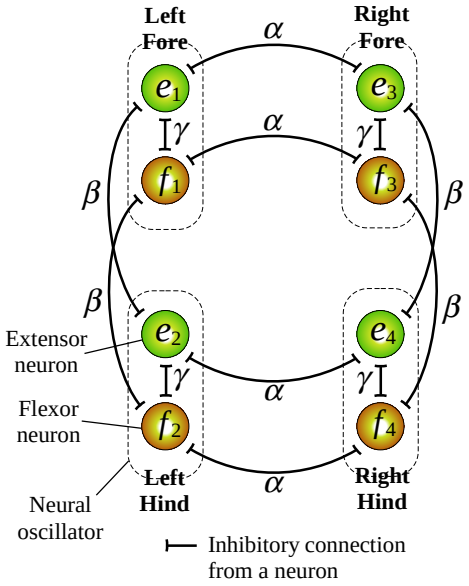

Figure 2: The mathematical CPG model prepared for our quadruped model. The diagram shows the four coupled neural oscillators enclosed by dashed lines. Each oscillator has an extensor neuron, e_i, and a flexor neuron, f_i. The suffix i represents the leg number, where 1 is the left foreleg, 2 is the left hindleg, 3 is the right foreleg, and 4 is the right hindleg. The paired neurons per leg are mutually inhibited to each other through a coefficient of connection, γ. The neurons are interconnected contralaterally and ipsilaterally via coefficients of connection α and β, respectively. This CPG model produces a trot pattern.

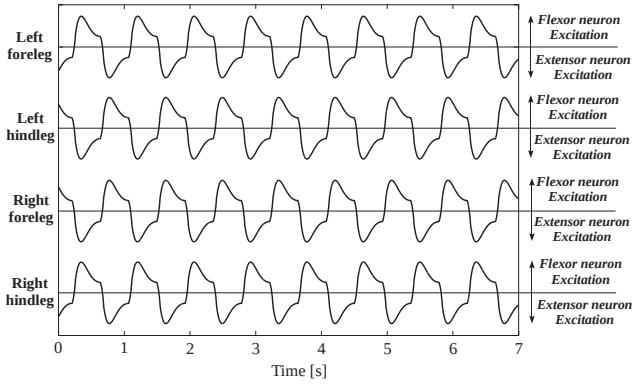

Figure 3: An example output from the neuron oscillator for each leg. This gait pattern shows a trot pattern.

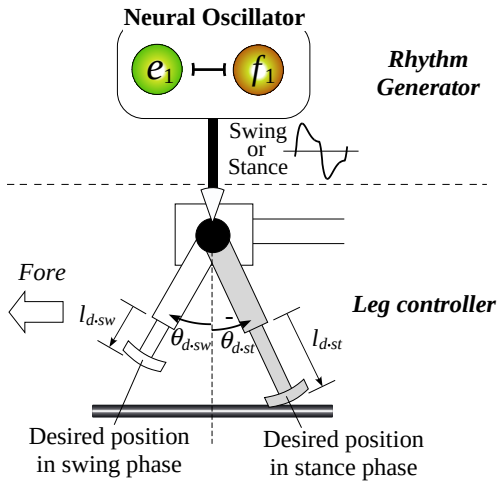

Figure 4: A diagram depicting the rhythm generation and leg control for each leg. The top half of the figure shows the rhythm generator, while the bottom half shows the leg controller. Here, $l_{d\cdot sw}$ and $\theta_{d\cdot sw}$ denote the target length of the linear leg joint and the target angle of the hip joint in the swing phase, respectively, and $l_{d\cdot st}$ and $\theta_{d\cdot st}$ denote those in the stance phase.

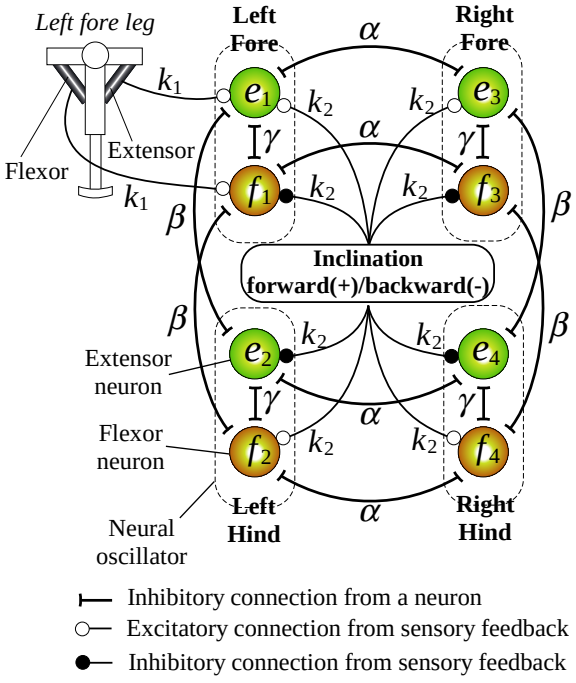

Figure 5: A diagram showing the mathematical CPG model used for our quadruped model. Two types of sensory feedback information are now included in the CPG model. First, the feedback of the extensor and flexor lengths of each leg to each neural oscillator is included through the weights, k_1, as shown in the figure on the top left. Second, the feedback of the body inclination to the neural oscillators is included through the weights, k_2, as shown in the middle.

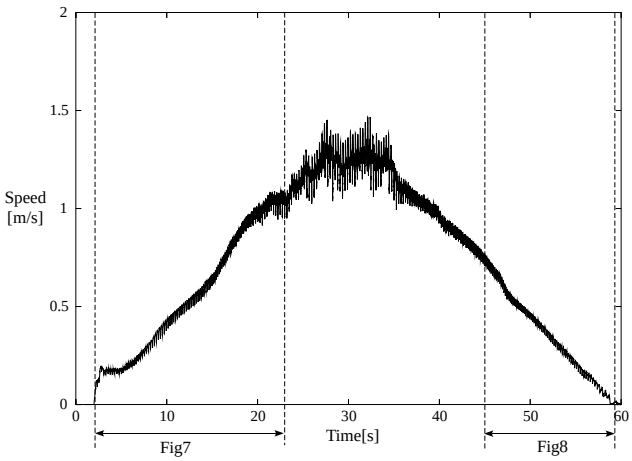

Figure 6: A graph of the speed while safely trotting for the quadruped model without vestibular modulation ($k_2 = 0$ in Fig. 5). The acceleration and deceleration were controlled to approximately $\pm$ 0.05 m/s^2. Specific simulation results for the speed up for 3 s to 23 s and the slow down for 45 s to 59 s are shown in Figs. 7 and 8, respectively.

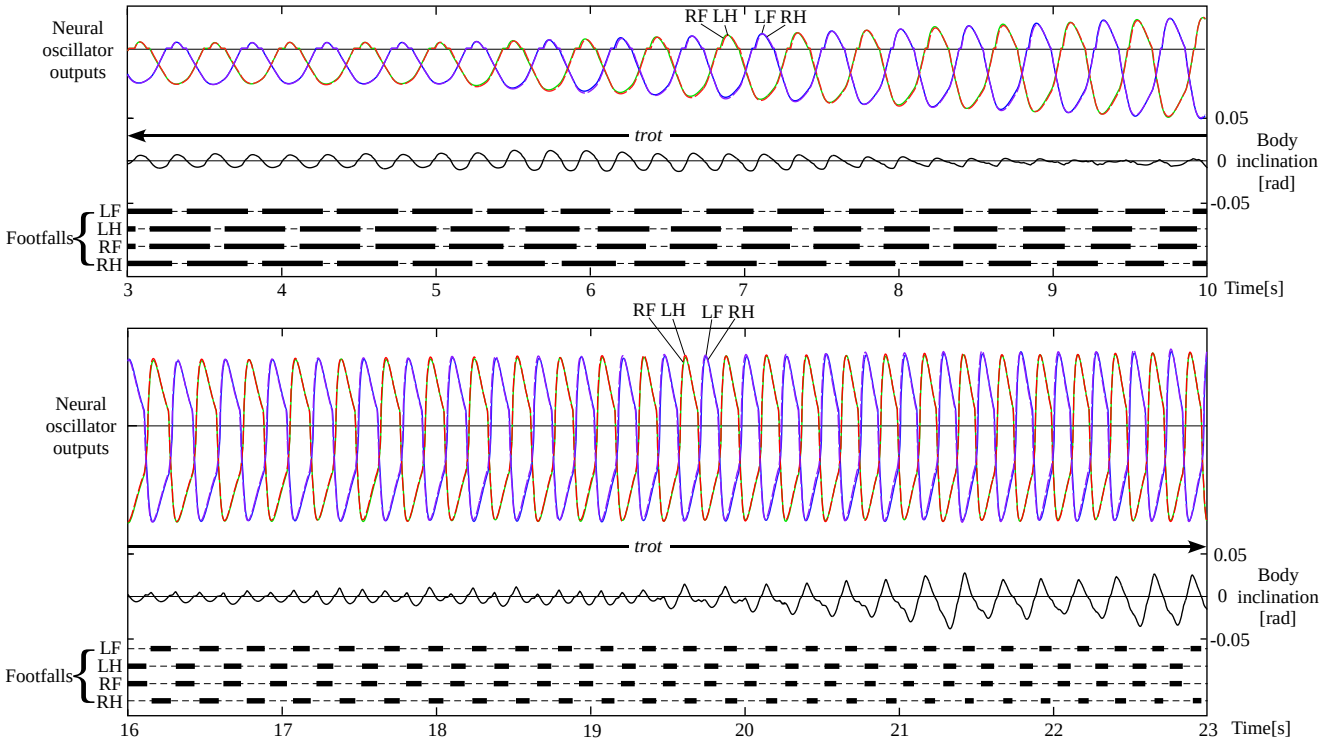

Figure 7: Simulation results for the quadruped model without vestibular modulation ($k_2 = 0$ in Fig. 5), for the acceleration between 3 s to 23 s shown in Fig. 6. LF, LH, RF, and RH are left foreleg, left hindleg, right foreleg, and right hindleg, respectively. The top oscillations indicate the neural oscillator outputs for the LF (blue), LH (red), RF (green), and RH (purple). The solid and dashed lines show fore and hindlegs, respectively. The middle waves show the body inclination (positive while tilting forward). The thick line segments on the thin dashed lines at the bottom show each leg's footfalls. The model is seen to be trotting continuously.

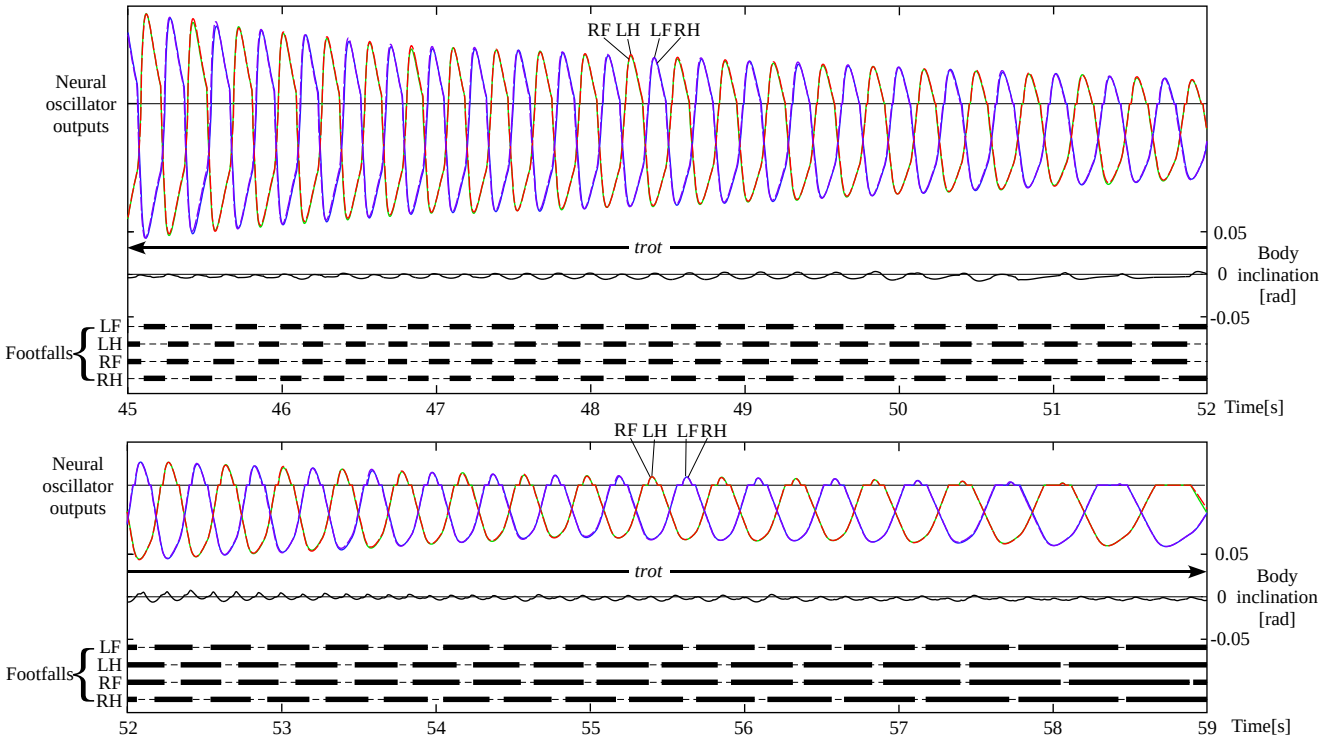

Figure 8: Simulation result for the quadruped model without vestibular modulation ($k_2 = 0$ in Fig. 5) for the deceleration between 45 s to 59 s of Fig. 6. The definitions for the plots are the same as for Fig. 7. The model is also seen to be trotting continuously.

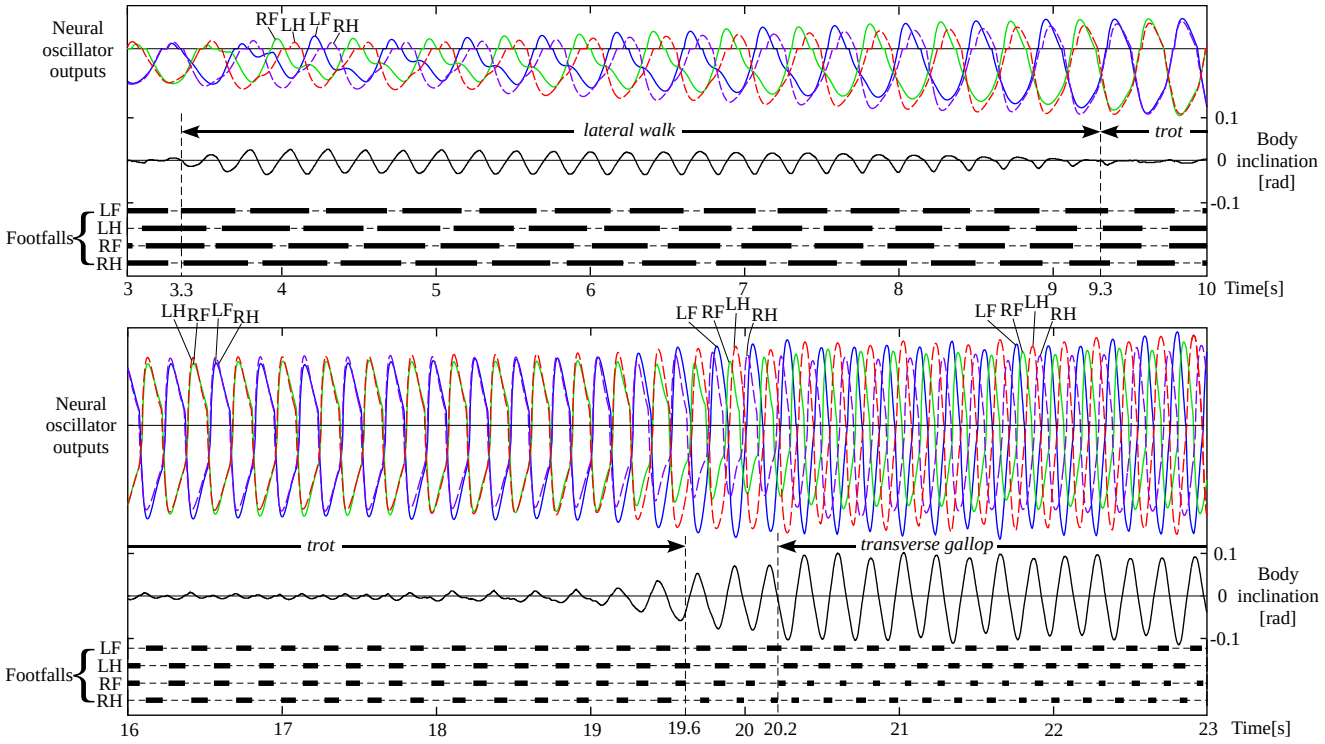

Figure 9: Simulation results for the quadruped model with vestibular modulation (k_2 is a fixed value in Fig. 5) during acceleration. The definitions of the plots are the same as those in Fig. 7. Note that the scale of the body inclination is different from those in Figs. 7 and 8. It should also be noted that the lateral walk and the transverse gallop appear at slow and high speeds (running), with a trot observed at a medium speed, even though the parameter values are identical to those in Figs. 7 and 8, with the exception of k_2.

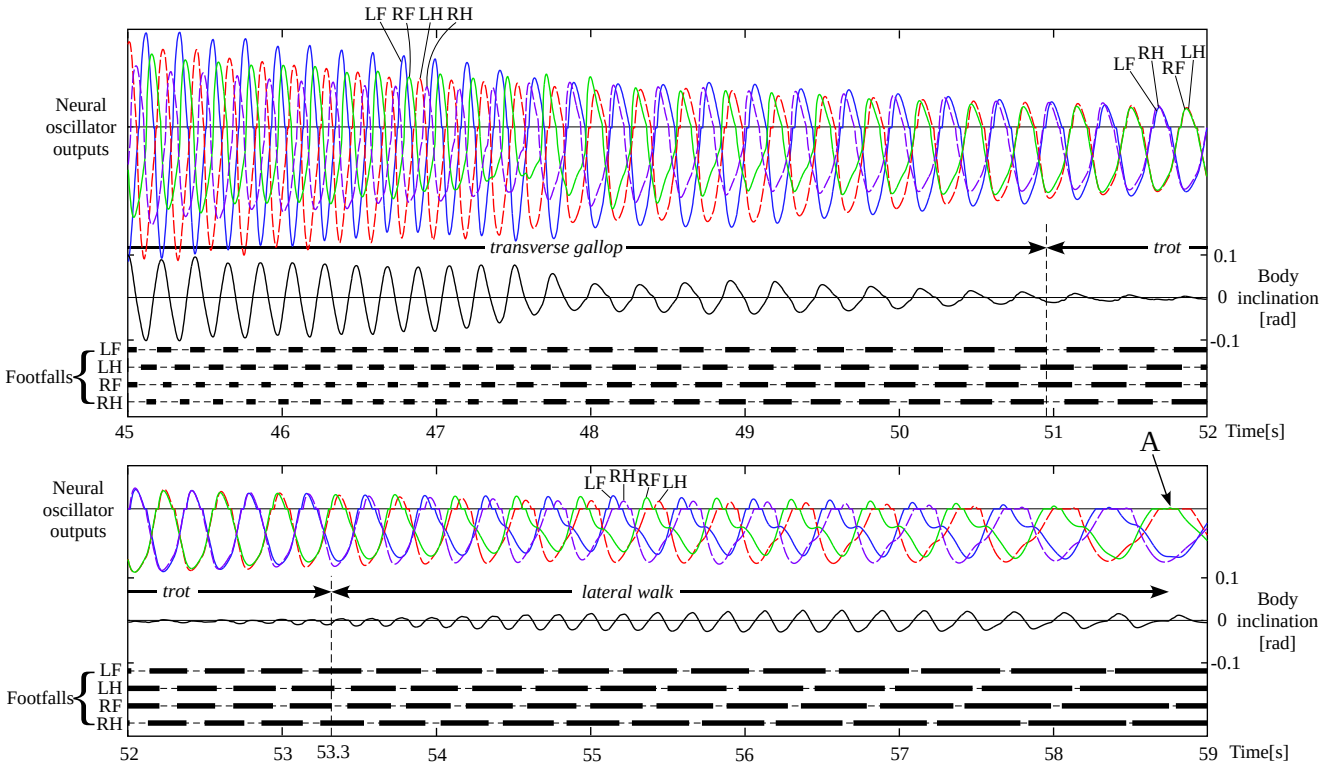

Figure 10: Simulation results for the quadruped model with vestibular modulation (k_2 is a fixed value in Fig. 5) during deceleration. The definitions of the plots are the same as in Fig. 7. Similarly to Fig. 9, the transverse gallop and the lateral walk appear at high (running) and slow speeds, while a trot appears for a medium speed.

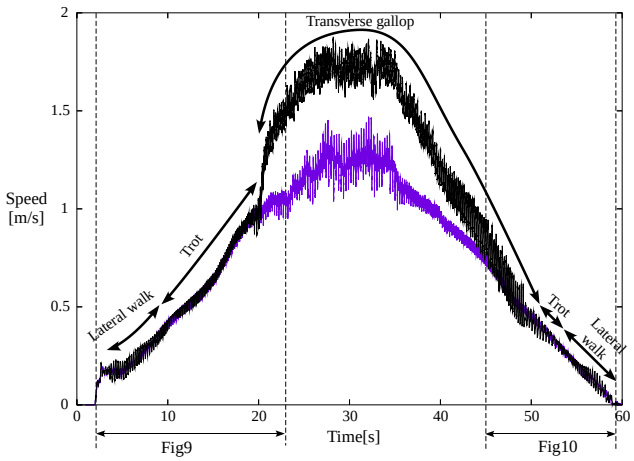

Figure 11: A plot of the speed of the quadruped model with vestibular modulation (k_2 is a fixed value in Fig. 5), shown in black. The result from Fig. 6 is also shown purple for comparison. Note that the speed shown by the black line is much greater during a transverse gallop than the speed of the purple line. The specific simulation results during acceleration from 3 s to 23 s, and deceleration from 45 s to 59 s, are shown in Figs. 9 and 10, respectively.

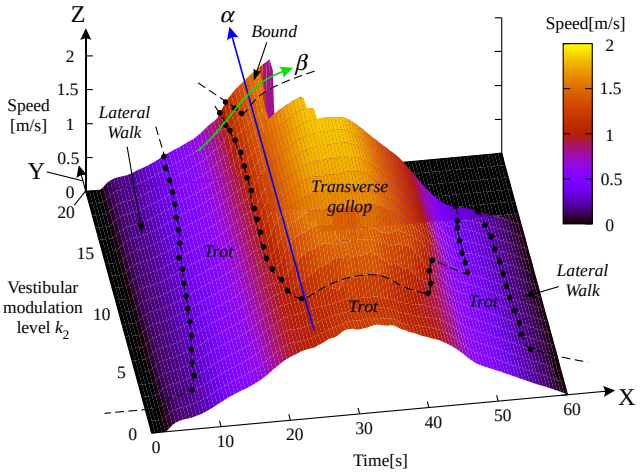

Figure 12: Simulation results for the quadruped model when varying the value for k_2 between 0 and 20. The same values for the speed control parameters as in the previous simulations were used. The X-, Y-, and Z-axes represent time, the vestibular modulation level k_2, and speed, respectively. The color meter on the right side shows the speed level. The color changes from black to yellow as the speed increases from 0 to 2 m/s. The observed gaits are marked on the figure, divided by the boundaries of the dots and four dashed lines. The arrow α indicates the gait changes from trotting to transverse galloping to bounding, due to the change of the value of k_2 at approximately 23 s. The arrow β shows the gait transition from trotting to transverse galloping to bounding according to the speed when k_2 is in the range 18 to 20.

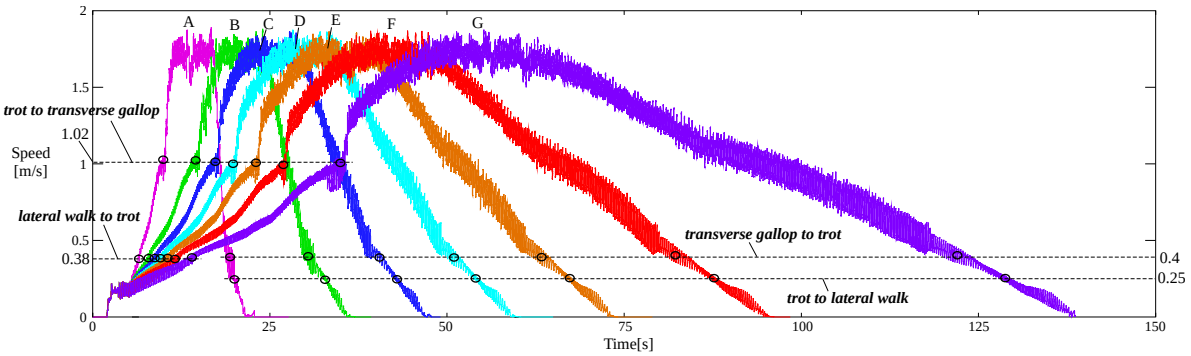

Figure 13: A variety of speed plots for varying acceleration/deceleration values in the locomotion of the quadruped model with vestibular modulation, for A: pink, B: green, C: blue, D: light blue, E: orange, F: red, and G: purple, where A-G are described in the main text. The moment where each gait transition occurs is marked with a ∘. Note that the speed transition between a trot and a transverse gallop is relatively abrupt in all curves, and that the speed at the moment of each gait transition is fairly constant.

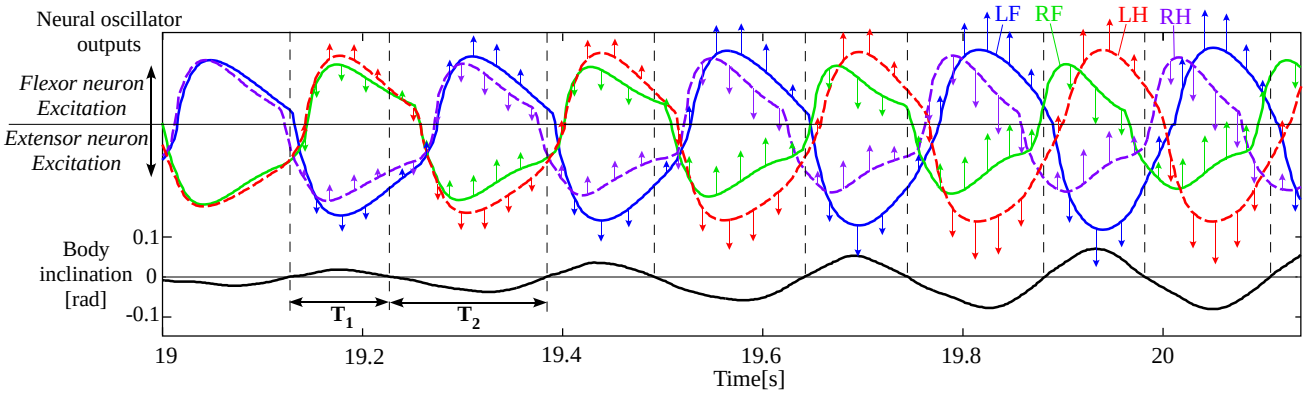

Figure 14: Plots of the neural oscillator outputs and the body inclination during the gait transition from a trot to a transverse gallop, extracted from Fig. 9. The abbreviations LF, LH, RF, and RH are as stated in Fig. 7. The top oscillations indicate the neural oscillator outputs of the LF (blue), LH (red), RF (green), and RH (purple). The solid and dashed lines show fore and hindlegs, respectively, and the bottom curves show the body inclination (positive while tilting forward). The periods T_1 and T_2 demonstrate two cases where the body is tilting forward and backward, respectively. The phases of the oscillator outputs were adjusted by the vestibular modulation as directed by the arrows, shifting the resulting gait from a trot to a transverse gallop.

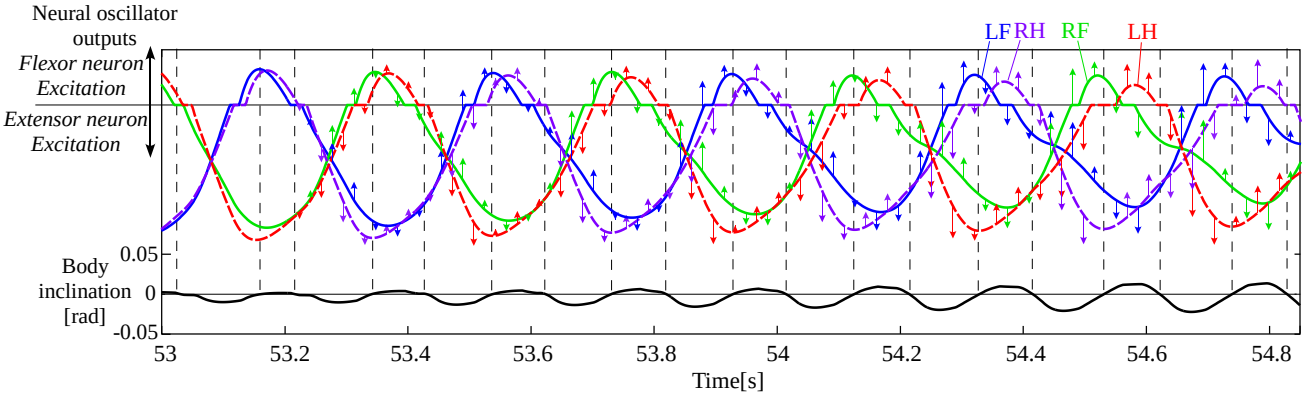

Figure 15: Plots of the neural oscillator outputs and the body inclination during the gait transition from a trot to a lateral walk, extracted from Fig. 10. The definitions of the symbols and plots are the same as in Fig. 14.

Appendix

The neural oscillator model used for each leg of our quadruped models was governed by the following set of differential equations. These equations are based on Matsuoka's neural oscillator model [Matsuoka, 1985, Matsuoka, 1987]:

$$\begin{aligned} T_r\dot{u}_{ei} + u_{ei} &= -\sum_{j=1}^{4}(p_{ij}[u_{ej}]^+ + q_{ij}[u_{fj}]^+) + s \\ &\quad -bv_{ei} + feed1_{ei} + feed2_{ei}, \quad (1) \\ T_a\dot{v}_{ei} + v_{ei} &= y_{ei}, \quad (2) \\ y_{ei} &= [u_{ei}]^+ = \max\,(u_{ei}, 0), \quad (3) \\ T_r\dot{u}_{fi} + u_{fi} &= -\sum_{j=1}^{4}(p_{ij}[u_{fj}]^+ + q_{ij}[u_{ej}]^+) + s \\ &\quad -bv_{fi} + feed1_{fi} + feed2_{fi}, \quad (4) \\ T_a\dot{v}_{fi} + v_{fi} &= y_{fi}, \quad (5) \\ y_{fi} &= [u_{fi}]^+ = \max\,(u_{fi}, 0), \quad (6) \end{aligned}$$

$$P_{i,j} = \begin{bmatrix} 0 & \beta & \alpha & 0 \\ \beta & 0 & 0 & \alpha \\ \alpha & 0 & 0 & \beta \\ 0 & \alpha & \beta & 0 \end{bmatrix}, Q_{i,j} = \begin{bmatrix} \gamma & 0 & 0 & 0 \\ 0 & \gamma & 0 & 0 \\ 0 & 0 & \gamma & 0 \\ 0 & 0 & 0 & \gamma \end{bmatrix} \quad (7)$$

, and

$$y_i = y_{fi} - y_{ei}, \quad (8)$$

where the suffix i denotes the number of leg (i.e., 1: left fore; 2: left hind; 3: right fore; 4: right hind); the suffixes e and f mark the extensor and flexor, respectively. The terms u_{ei} and u_{fi} indicate an inner state modeled on a membrane potential of the extensor and flexor neurons of the ith leg, respectively, and v_{ei} and v_{fi} indicate the variable representing the degree of fatigue or adaptation in the extensor and flexor neurons of the ith leg, respectively. Meanwhile, s is a tonic descending signal strength; $feed1_{\{e,f\}i}$ and $feed2_{\{e,f\}i}$ represent sensory feedback inputs (e.g., $feed1_{ei}$ is a feedback to the extensor neuron of the ith leg); y_{ei} and y_{fi} are the outputs of the extensor and flexor neurons of the ith leg, which are discontinuous terms via Eqs. (3) and (6); and y_i is the output of the oscillator of the ith leg, as shown by the patterns in Fig. 3 in the main text. The constants T_r and T_a are time constants of the inner state and the adaptation variable to determine the intrinsic frequency of the oscillator, and b is a constant related to the recurrent inhibition of the inner state. Finally, $\sum_{j=1}^{4}(p_{ij}[u_{\{e,f\}j}]^+ + q_{ij}[u_{\{f,e\}j}]^+)$ represents the inhibitory synaptic inputs from the neurons of the legs, such as in Fig. 5 in the main text, where their strengths p_{ij} and q_{ij} are shown in Eq. (7). The essential gait pattern is produced by this term.

The sensory feedback inputs in Eq. (1) and Eq. (4) are defined as

$$\begin{aligned} feed1_{ei} &= k_1(\theta_i - \theta_0), \text{ and} \\ feed1_{fi} &= -k_1(\theta_i - \theta_0) \end{aligned} \quad (9)$$

where k_1, θ_i and θ_0 are the weight, the present hip joint angle of the ith leg, and the origin of each hip joint angle, respectively, as shown in Fig. 16. Next:

$$\begin{aligned} feed2_{ei} &= \sigma(leg)\ k_2\phi, \text{ and} \\ feed2_{fi} &= -\sigma(leg)\ k_2\phi \end{aligned} \quad (10)$$

and:

$$\sigma(leg) = \begin{cases} 1, & \text{if } leg \text{ is a foreleg } (i{=}1 \text{ or } 3); \\ -1, & \text{if } leg \text{ is a hindleg } (i{=}2 \text{ or } 4) \end{cases}$$

where ϕ denotes a body inclination angle around the pitch axis as shown in Fig. 16, and k_2 is the strength of vestibular modulation.

The equations of the proportional-derivative (PD) controllers used in the leg controller section in Fig. 4 in the main text will now be introduced. The PD control of each hip joint is shown as:

$$\tau_i = K^{\tau}_{pi\cdot\{sw,st\}}(\theta_{di\cdot\{sw,st\}} - \theta_i) - K^{\tau}_{vi\cdot\{sw,st\}}\dot{\theta}_i, \quad (11)$$

where τ_i, θ_i and $\dot{\theta}_i$ are the output torque, the present angle, and the present angular velocity of the hip joint of the ith leg in Fig. 16, respectively. The terms $\theta_{di\cdot\{sw,st\}}$ are the target hip joint angles in the swing/stance phase (Fig. 4 in the main text), and $K^{\tau}_{pi\cdot\{sw,st\}}$ and $K^{\tau}_{vi\cdot\{sw,st\}}$ represent proportional and derivative gains (P and D gains) in the swing/stance phase. The PD control of each linear knee joint is shown as:

$$F_i = K^{F}_{pi\cdot\{sw,st\}}(l_{di\cdot\{sw,st\}} - l_i) - K^{F}_{vi\cdot\{sw,st\}}\dot{l}_i, \quad (12)$$

where F_i, l_i and $\dot{l}_i$ are the output force, the present length, and the present velocity of the linear knee joint of the ith leg in Fig. 16, respectively; $l_{di\cdot\{sw,st\}}$ are the target lengths of the linear knee joints in the swing/stance phase (Fig. 4 in the main text), and $K^{F}_{pi\cdot\{sw,st\}}$ and $K^{F}_{vi\cdot\{sw,st\}}$ represent P and D gains in the swing/stance phase.

The values of the parameters in the equations were empirically determined such that the quadruped model could walk and run safely at each chosen speed. For a selected speed, all the values are constant. However, the values of s, T_r, $\theta_{d\cdot st}$, $K^{\tau}_{pi\cdot st}$, $K^{F}_{pi\cdot st}$ and $K^{F}_{pi\cdot sw}$ are set according to the selected speed. All other values are constant irrespective of changes in the speed. For example, we show the values of the parameters in Table 1 when the quadruped model is walking with a walk gait at 0.3 m/s.

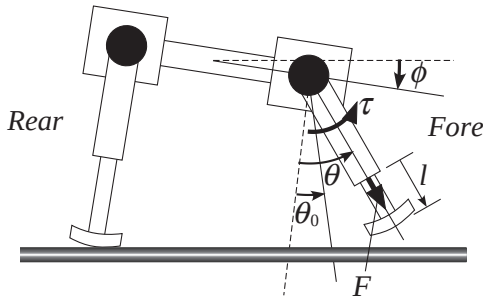

Figure 16: A diagram of the quadruped model.

Table 1: Values of the parameters used in a simulation where the quadruped model is walking with a walk gait at 0.3 m/s.

Parameter	Value	Parameter	Value
T_r	0.0575	$\theta_{di\cdot sw}$	0.873 rad
T_a	0.6	$\theta_{di\cdot st}$	0.218 rad
s	1.55	$K^{\tau}_{pi\cdot sw}$	5.0 Nm/rad
b	3.0	$K^{\tau}_{vi\cdot sw}$	1.0 Nms/rad
α	-0.6	$K^{\tau}_{pi\cdot st}$	5.03 Nm/rad
β	-0.57	$K^{\tau}_{vi\cdot st}$	1.0 Nms/rad
γ	-2.0	$l_{di\cdot sw}$	60 mm
θ_0	-0.262 rad	$l_{di\cdot st}$	120 mm
k_1	3.0	$K^{F}_{pi\cdot sw}$	1775.0 N/m
k_2	9.3	$K^{F}_{vi\cdot sw}$	45.0 Ns/m
		$K^{F}_{pi\cdot st}$	876.0 Nm/m
		$K^{F}_{vi\cdot st}$	20.0 Ns/m